Proteomic analysis of PEG-fractionated UV-C stress-response proteins in globe artichoke

Proteomic analysis of PEG-fractionated UV-C stress-response proteins in globe artichoke

Sara Falvo [a,b], Alberto Acquadro [a,†], Alessandra Giuliano Albo [b], Twan America[c], and Sergio Lanteri [a]

[a] *DiVaPRA, University of Turin, via L. da Vinci 44, 10095 Grugliasco (TO), Italy.*

[b] *L.I.M.A. Bioindustry Park Silvano Fumero, via Ribes 5, 10010 Colleretto Giacosa (TO), Italy.*

[c] *Plant Research International, Droevendaalsesteeg 1B, 6708PB, Wageningen, The Netherlands.*

†Corresponding author

Alberto Acquadro

Phone: +39 (0)11 6708813

Fax: +39 (0)11 2368813

Mail: alberto.acquadro@unito.it

Keywords

Abiotic stress, globe artichoke, PEG fractionation, proteomics

Abstract

Plants respond to UV stress by producing antioxidant molecules and by altering their metabolism through the regulation of specific gene family members. Globe artichoke (*Cynara cardunculus* var. *scolymus* L. - *Compositae* family) is an attractive model species for studying the protein networks involved in UV response, being characterized by high loads of antioxidants, which are boosted by UV-C rays.

The effect of UV-C on leaf proteome was investigated 24 hours after irradiation by applying a PEG fractionation method, which we previously developed to cope with the so-called high abundance protein, followed by 2-DE analysis. Thirty-eight UV-C modulated proteins were analysed by means of Nano-LC-nanospray MS/MS and 27 were succesfully identified using a customised *Compositae* protein database, including a set of 19055 globe artichoke unigenes. Proteins were categorised according to Gene Ontologies (GO), and visualized on their cellular pathway: most of them were involved in primary metabolism (e.g.: photosynthesis) and in abiotic stress responses (e.g. ROS scavenging) but also in cell wall modification, secondary metabolism, and regulation of transcription.

To date, this is the first report on globe artichoke proteomic expression analysis following abiotic stress. Our results confirm the effectiveness of the PEG fractionation method in excluding most of the ribulose bisphosphate carboxylase/oxygenase (RuBisCO), and highlighting some major occurring phenomena.

Introduction

UV radiation is hazardous to living organisms (Coohill 1999): the highly energetic photons are able to destroy chemical bonds of biomacromolecules, leading to an array of cell injuries: lipid peroxidation, membrane damage impairing transport system, as well as alteration of amino acids and enzyme inactivation (Stapletons 1992). Plants respond to UV stress by altering their metabolism through the regulation of specific gene family members and by producing antioxidant molecules, which can act as sunscreens and are also responsible for a variety of therapeutic effects in human beings (Wang et al. 2003).

Globe artichoke (*Cynara cardunculus* var. *scolymus* L.) represents a very interesting model species to study this phenomenon since it is characterized by very high loads of antioxidant molecules (e.g. polyphenols). Actually, it has been shown that polyphenols are greatly boosted in UV-C irradiated globe artichoke leaves, and reach their maximum level at 24h (Moglia et al. 2008). A proteome survey in globe artichoke is thus crucial to understand the molecular processes involved in UV-C response in our species. Proteomic tools have been widely used in plants to survey protein variations following biotic (Zhang et al. 2010, Qian et al. 2010) and abiotic (Ding et al. 2011, Jellouili et al. 2010) stresses. However, a documented drawback of two-dimensional electrophoresis (2-DE) is the failure in identifying low abundance or hidden proteins (Righetti and Boschetti 2007). To overcome this problem, we previously developed a reproducible PEG fractionation procedure (Acquadro et al. 2009), which consistently reduce the abundant RuBisCO content and contribute to improve the isolation of masked proteins

In this work, the optimised PEG fractionation method, coupled with 2-DE and Nano-LC-nanospray MS/MS analysis, has been applied for the first time in globe artichoke to highlight the proteome variation following UV-C irradiation: the functional role of the modulated proteins is discussed.

Materials and methods

Plant material

Seeds of globe artichoke F1 hybrid 'Concerto' (Numhems) were germinated on wetted filter paper and held for two weeks at 20°C under a 16h day/8h night regime (light intensity 120 µmol m^{-2} s^{-1}). Seedlings were transplanted to 10 cm diameter pots containing sterile potting mixture consisting of Brill type 3 special (Brill, Maubec, France), and transferred to a greenhouse. After about ten weeks, the fully expanded sixth leaves were collected for stress application.

UV-C treatment and HPLC analysis

In a preliminary experiment four technical replicates were performed showing a not significant technical variability, as we previously reported (Acquadro et al. 2009) . The experiments were thus carried out using 4 biological replicas. From each independently collected leaf, 8 foliar disks (diameter: 2 cm) were produced. Four of them were exposed to UV-C light (254 nm) for 20 min, through a 16 W germicidal lamp (Koninklijke Philips Electronics N.V, N.Y. US), at a distance of 20 cm from the light source (3,2 mW/cm2), as described by Moglia et al. (2008); four control disks were subjected to the same procedure, maintaining the lamp off (Figure 1A). Treated/untreated foliar disks were derived from the same area of the leaf. After the treatment, samples were maintained under a 16h light/8h dark regimen, in double distilled water. Twenty-four hours after the treatment, disks from each leaf were harvested, pooled and grounded in liquid nitrogen.

Leaf powder was weighted (100mg) and metabolites were extracted with three volumes of pure methanol (0.1% formic acid). The mixture was sonicated in a water bath for 20 min, and centrifuged at 16,000 x g for 10 min. The supernatant was filtered through a 0.45 µm Anotop 10 filter (Whatman) before injection into HPLC-PDA (Waters, USA) following the procedure described by Moglia et al.(2008). Briefly, a Luna C18 (2) precolumn (2 × 4 mm) and an analytical column (2 × 150 mm, 100 Å, particle size 3 µm) were used for the chromatographic separation. The mobile phases consisted of trifluoroacetic acid/ultrapure water (1:1000, v/v) as eluent A; and trifluoroacetic acid/acetonitrile (1:1000, v/v) as eluent B applying the following gradient system: initial, 5% B; linear gradient to 35% B in 45 min, with a flow rate of 1 mL/min; the injection volume was 10 µL, and the detection wavelength was recorded at 240-600 nm. The identification of metabolites was based on the following parameters: 1) retention time, 2) UV/VIS spectral information and 3) comparison with reference standards. Quantification of dCQAs was performed by comparison to standard 1,5-dicaffeoylquinic acid from Chengdu Biopurify Phytochemicals Ltd (China).

Protein extraction and PEG fractionation

The protein extraction and PEG fractionation protocols (Acquadro et al. 2009) were performed as depicted in Figure 1B. Globe artichoke powdered leaves (2 gr) were homogenized in 10 mL of cold Mg/NP-40 buffer: 0.5 M Tris-HCl pH 8.3, 2% v/v NP-40, 20 mM $MgCl_2$, 2% v/v β-mercaptoethanol, 1% v/v protease inhibitor cocktail (Sigma-Aldrich, Saint Louis), 1% w/v polyvinylpolypyrrolidone (PVP). The slurry was centrifuged at 12,000 x g for 15 min at 4°C to obtain a cell-free supernatant, to which 0.2 volumes of 50% (w/v) PEG solution (PEG 6000, AppliChem) were added. After stirring at 4°C for 30 min, the slurry was centrifuged at 1,500 x g for 10 min at 4°C. The supernatant was made to 20% w/v PEG by adding the required volume of 50% (w/v) PEG solution, incubated for 30 min at 4°C, and centrifuged at 12,000 x g for 15 min at 4°C. The remaining supernatant was precipitated using the TCA/acetone method (Damerval et al. 1986) and the pellet dissolved in UTC buffer (7M Urea, 2M Thiourea, 4% CHAPS). The protein extract was re-centrifuged at 20,000 x g to remove insoluble cell debris, the supernatant purified using Clean-Up kit (GE Healthcare) and the pellet resuspended again in UTC buffer. Prior to the 2-DE procedure, the protein content in each sample was measured by the Bradford method (Bradford 1976). Four indipendent extractions, from four plant individuals, were performed for each group.

2-DE analysis

About 100 μg of each sample were mixed with 2% v/v immobilized pH gradient (IPG) buffer (pH 3-10, GE Healthcare), 60 mM dithiothreitol (DTT), 0.4% w/v bromophenol blue, loaded on to an 18 cm pH 3-10 non-linear gradient IPG strip, and separated on an IPGPhor Unit (GE Healthcare), using the Ettan IPGPhor Manifold. The experimental samples were isoelectrofocused together in the same run, to reduce technical variability. The IPG strips were then incubated in 4 mL of equilibration buffer (6 M urea, 30% w/v glycerol, 2% w/v SDS, 0.002% w/v bromophenol blue, 50 mM Tris-HCl pH 8.8) containing 1% w/v DTT for 15 min, and subsequently in 4 mL of the same buffer containing 2.5% w/v iodoacetamide (IAA) for 15 min and subjected to SDS-PAGE in a 12.5% polyacrylamide gel adopting the running conditions reported in Bian et al. (2010). The 2-DE gels were stained with Sypro Ruby (BioRad's) following manufacturer's instructions. Preparative gels were obtained loading 1 mg of protein extract, using the same settings, and stained with Coomassie blue R-350 (GE Healthcare) (Albo et al. 2007).

Image scanning and data analysis

Sypro stained gel images were scanned using a ProXPRESS 2-D CCD camera (Perkin Elmer Life Sciences, Boston, MA, USA) with the following parameters: excitation 460/80, emission 650/50 and 100 μm resolution. The images were analysed using ImageMaster™ 2-D Platinum software

v6.0 (GE Healthcare), according to the manufacturer's instructions. Percentage volumes of the matched spots were exported in Excel files, log-transformed and subjected to the statistical analysis. One-way ANOVA was performed using statistiXL Version 1.x software (http://www.statistixl.com), applying the false dicovery rate (FDR). Changes in protein spots were considered as UV-C modulated when the following criteria were met: (i) a p-value cutoff of 0.05; (ii) a fold change threshold of 1.50; and (iii) spot presence in the 80% of the maps.

Identification of proteins by MS/MS

UV-C modulated spots were manually picked up from preparative gels. In-gel digestion, reduction and alkylation of proteins were performed as described by Shevchenko et al. (2006) and nano LC-nanospray MS/MS analyses was performed loading 1 µl of each sample onto a ZORBAX 300 SB C18 RP column (75 µm x 150 mm, 3.5 µm particles, Agilent Italia, Milan, Italy). Peptides were eluted with a gradient of acetonitrile from 5% to 80% (containing 0.1% formic acid) at a flow rate of 0.3 µl/min by a HP 1100 nanoHPLC system coupled to a XCT-Plus nanospray-ion trap mass spectrometer (Agilent Italia, Milan, Italy). MS parameters were the following: scan range m/z = 100-2200, scan speed 8100 m/z s−1, dry gas flow 5 L/min, dry temperature 300°C, capillary 1.8 kV, skimmer 40 V, ion charge control (ICC) target 125000, maximum accumulation time 300 ms. Positively charged peptides ions were automatically isolated and fragmented, and spectra were deconvoluted by the DataAnalysis software (Bruker Daltonics, Bremen, Germany).

Mascot Daemon v2.2.2 (Matrix Science, London, UK) was employed for protein identification, searching against a customized database, representative of the *Compositae* family. Contig databases from *Cynara cardunculus* (Scaglione et al. 2009), *Lactuca sativa* (status 16 July 2008), *Lactuca serriola* (status 01 July 2008), *Heliantus annuus* (status 29 May 2009) and *Hevea* spp. (status 5 june 2009) have been downloaded from NCBI (http://www.ncbi.nlm.nih.gov/) and TGI (http://compbio.dfci.harvard.edu/tgi/) databases and the nucleotide sequences were translated into amino acid sequences by using NucToProt tool, (in-house software developed at Plant Research International - PRI, Wageningen, NL). FastaFileMerger (in-house software developed at PRI) was used to merge the downloaded databases along with a keratin-trypsin database subset, and to reduce the redundancies (based on 100% sequence similarity parameter). The database contained 143,516 protein accessions (N50 = 205 amino acids, average length = 156 amino acids). The merged *Compositae* protein database was uploaded in Mascot Daemon and a search was performed using the following parameters: (i) trypsin: one missed cleavage allowed, (ii) fixed modification: carbamidomethyl (C), (iii) variable modifications: deamidated (NQ) and oxidation (M), (iv) peptide tolerance tolerance: ± 1.2 Da, (v) MS/MS tolerance: ± 0.6 Da, (vi) peptide charge: +1, +2, +3 (monoisotopic), (vii) instrument type: ESI-TRAP. Only significant hits, as defined by the MASCOT probability analysis ($p \leq 0.05$), were accepted.

GO terms annotation and pathway visualization

Gene Ontology terms for molecular function, biological process, and cellular components were derived from the Blast2GO v.2.3.6 bioinformatic tool (www.blast2go.org), following the workflow suggested by Conesa et al. (2005) to retrieve enzyme codes (E.C. numbers) and protein annotation (adopting *Arabidopsis* as model). Pie chart graphs were produced in order to summarise the distribution of the whole protein set involved in UV-C stress response.

MapMan software v3.0 was downloaded from GABI Primary Database (http://mapman.gabipd.org/web/guest/home) and manual's instructions were followed to produce customized globe artichoke biochemical pathways. Briefly, the *Compositae* protein database was taken as template and submitted to Mercator tool (http://mapman.gabipd.org/web/guest/app/mercator) to produce a customized 'ontology/mapping file' where *Compositae* proteins were organised in a set of hierarchical functional categories (BINs, subBINs, individual enzymes). Subsequently, subBINs were manually introduced to differentiate protein isoforms and allow for their visualisation on the MapMan pathways. The 'experimental file', a table containing the protein fold changes, as well as the 'mapping file' were uploaded in MapMan and UV-C responsive proteins visualized on metabolic pathways.

Results and Discussion

Metabolite and PEG-enriched leaf proteome analyses after UV-C treatment

2-DE has been widely applied to investigate how plants respond to biotic and abiotic stresses; in particular, many studies have been performed to address for UV-B stress, adopting different plant species and stress conditions (Casati et al. 2005; Xu et al. 2008; Kaspar et al. 2010; Singh et al. 2010; Du et al. 2011). UV-C radiation has been applied (Figure 1) as a convenient source of light stress in globe artichoke, since it has been generally considered to have similar, but more intense effects as compared to UV-B (Moglia et al. 2008). The efficacy of the UV-C treatment was confirmed by monitoring the quantitative induction of dCQAs in globe artichoke leaves after 24h from the stimulus: UV-C exposed foliar disks showed a four fold increase (93,2 ± 27,2 mg/100g fw) than control ones (25,2 ± 1,31 mg/100g fw). These results confirmed the dCQAs accumulation and their role as marker of stress, following UV-C stimulus, as previously reported (Moglia et al. 2008) [4].

In order to obtain 2-DE maps for total and PEG fractionated leaf proteins a protein extraction method, modified for globe artichoke leaf tissue (Acquadro et al. 2009), was applied. As expected, the PEG fractioning significantly reduced the characteristic RuBisCO horizontal smearing (pI: about 5; MW: about 55 KD, data not shown), leading to a significant enhancement of the visualised protein spots (1.5 fold increasing) otherwise undetectable, thus, improving the analytical dynamic range and detection sensitivity.

PEG fractionated leaf proteins derived from treated/untreated leaves were analysed by 2-DE (Figure 1C). Approximately, 892 average matched protein spots, pI between 3 and 10 and Mw between 10 and 200 kDa, were reproducibly resolved by 2-DE with an average coefficient of variation (CV) of 18%. The protein patterns of untreated and UV-C exposed leaves were compared (Figure 2, Table 1) and the image and statistical analysis revealed 38 differentially expressed proteins, of which 16 were up- and 22 down-regulated (Additional file 1).

Protein spot identification

Twenty-seven (71%) out of the 38 UV-C responsive proteins were succesfully identified (Figure 2, Table 1). Most of them were linked to different accessions of the *Compositae* protein database, and most of the matched peptides were shared among orthologs. In five cases (spots §144, 359, 473, 690, 1219), differences in orthologous peptides detected in spectra were found (Additional file 2), enabling to distinguish protein isoforms not still described in public databases. In some cases (spots §220, 240, 472, 473, 480, 514, 568, 639, 659), the same gene function was assigned to

multiple spots, presumably because of post-translational modifications, which may alter electrophoretic mobility. Two spots (§423 and 575) matched to multiple hits (Additional file 2), likely reflecting a co-migration of proteins or a cross-contamination during picking. In these cases, it was not possible to attribute a proper expression value and to infer any specific protein role in the stress response.

Protein functional roles

Gene Ontology pie charts and metabolism maps (Figure 3) were employed to describe the roles of the UV-C responsive proteins. Most of them were involved in primary metabolisms (Figure 3), in photosynthesis, stress responses and redox scavenging. However, proteins having a role in other metabolic pathways were also identified: namely, fructan and inulin metabolisms, cell wall modification, amino acid biosynthesis and regulation of transcription. Overall, the gene ontology analysis revealed a significant protein component (48.1%) involved in “abiotic and biotic stimulus” (GO:0009628; GO:0009607).

Our results on UV-C stress in globe artichoke are in accordance to what generally observed in plant (Singh et al. 2010; Du et al. 2011), where UV exposure resulted in a decrease in the photosynthetic rate, accumulation of UV-absorbing compounds or protein involved in defense mechanisms. Overall, as reviewed in Zolla et al. (2008) proteins primarily involved in early stress responses seem to be common among different abiotic stressors. Likely, plants have adopted general mechanisms of defense to suddenly deal with the "big problem” and to care afterwards about the “details.”

Photosynthesis

Many UV-C regulated enzymes were found to be located in chloroplasts (Figure 3) and involved in both “light“ and “dark” photosynthesis reactions (Figures 4A and 4B). As depicted in Figure 4A, one isoform of the oxygen evolving complex (OEC - 33kDa) of photosystem II (spot §1219), one of photosystem I (spot §996), as well as the ferredoxin $NADP^+$ oxido-reductase (spot §690) were found downregulated after 24h. This suggests a specific role of UV-C radiation into impairing the electron transfer chain as well as in damaging light-harvesting complex, responsible for capturing/delivering excitation energy (Dong et al. 2011) consequently converted in ATP/NADPH. On the contrary, enzymes involved in the Calvin cycle were found to be mainly up-accumulated 24h after UV-C exposure, as depicted in Figure 4B. Among them, two isoforms of phosphoglycerate kinase (PGK, spots §240 and 480), which regulates CO_2 fixation with respect to the cellular needs of ATP and NADPH were induced; indeed, PGK can contribute both to Calvin cycle and glycolysis and thus it was not possible to separate their specific contribute onto the UV-C perturbed system. Two isoforms (spots §220 and 514) of sedoheptulose-bisphosphatase (SBPase) were induced. SBPase catalyses the step where carbon gets committed to ribulose

bisphosphate (RuBP) regeneration, instead of starch synthesis. Its role in regulating carbon flow in the Calvin cycle has been investigated in tobacco transgenic plants (Miyagawa et al. 2001) and (Lefebvre et al. 2005), in which an increased SBPase activity stimulated photosynthesis and growth. Moreover, transgenic rice plants overexpressing SBPase showed an increase of photosynthesis even under high temperature stress, by maintaining the activation of RuBisCO and enhancing the tolerance to CO_2 assimilation (Feng et al. 2007). Spot §572, found to be induced following UV-C stress, was identified as phosphoribulose kinase (PRK), responsible for ribulose 5-phosphate phosphorylation in the last step of the Calvin cycle. Among the UV-C modulated Calvin cycle enzymes observed in globe artichoke, fructose 1,6-bisphosphate aldolase (FBP aldolase, spot §659) was the only one found to be repressed (Figure 4B). Triose phosphate isomerase (TIM) which catalyzes the reversible interconversion of glyceraldehyde 3-phosphate and dihydroxyacetone phosphate, thus regulating ATP production, was found to be less accumulated (spot §886).

Overall, UV-C radiation seemed to enhance the content of protein involved in the "dark" reactions of photosynthesis, whilst at the same time, to repress the protein directly engaged by the light stimulus ("light" reactions). In other words, light-stressed plant cells showed a tendency to re-establish cellular homeostasis driving up energy production (carbon assimilation for ATP synthesis) presumably in order to repair the electron transport chain and face the occurred cell damages.

Abiotic stress-related proteins

Many UV-C regulated enzymes were involved in "abiotic and biotic stimulus" (Figure 3). Hsp70 (spot §144) was found to be up-accumulated accordingly to the role of Heat Shock Proteins in maintaining enzymes in their functional conformations, preventing the aggregation of non-native proteins, as well as in re-establishing cellular homeostasis under stress conditions (Wang et al. 2004; Timperio et al. 2008). Hsp70 modulation was also observed in many studies addressed to UV stress analysis (Casati et al. 2005; Xu et al. 2008; Kaspar et al. 2010; Singh et al. 2010).

It has been demonstrated that increased levels of Hsp70 affect phenylpropanoid metabolism and is related to the accumulation of the enzyme phenylalanine ammonia lyase (PAL, Kuun et al. 2001). Presumably, although it has to be experimentally confirmed, Hsp70 accumulation might positively affect the whole channelled phenylpropanoid flux, due to the multiprotein complex organisation of this cytosolic pathway, closely linked to the endoplasmatic reticulum membrane (Winkel 2004).

Cysteine synthase (CS, spot §579), a key enzyme in cysteine biosynthesis, was strongly accumulated (fold change: 7.62) after UV-C treatment. Up-regulation of cysteine synthase following metal stress has been documented, so far (Yang et al. 2007); moreover, CS has been found markedly accumulated in response to both arsenate and H_2O_2 treatment in rice roots proteome (Ahsan et al. 2008), suggesting a role in ROS detoxification. Actually, when ROS levels

overcome the scavenging potential of cellular antioxidants, many sulfur-containing molecules such as CS are newly synthetised to preserve cell protection (Yang et al. 2007).

Xyloglucan endotransglucosylase/hydrolase (XTH), involved in cell wall modification, was repressed 24h after UV-C stress (spot §751). XTH has been found to be up-regulated by touch stimulus, darkness, heat shock, cold (Braam and Davis 1990; Braam 1992; Polisensky and Braam 1996), drought and ethylene (Cho et al. 2006), brassinosteroids (BRs) and indole-3-acetic acid [IAA] (Iliev et al. 2002). Up to now, no evidences of XTH light stress regulation are available and, interestingly, our study evidenced a negative UV-C light modulation which is consistent with XTH behaviour in darkness (Braam 1992). Reduced XTH levels might have been thus altered by changes in protein degradation, post-transcriptional or other regulation mechanisms.

The spot §848, identified as acidic endochitinase, showed a 5-fold up-modulation. Chitinases are pathogenesis-related (PR) proteins, generally involved in biotic defense reactions, but also induced by various abiotic factors (Li et al 2010, Kasprzewska 2003) including elicitors, wounding, salicylic acid, inorganic salts, ethylene, auxin, cytokinin, ozone and UV light. Consistently, the class III chitinase IF3 of *Lupinus albus* was found to be induced both at mRNA and protein level, following *Colletotrichum gloeosporioides* infection as well as in response to UV-C light and wounding (Regalado 2000). Recently, UV-C irradiation effect on chitinases (class I and III) gene expression was investigated in grapevine (Petit et al. 2009) and an enhanced activity was observed in bunch stems (peduncle and pedicels).

The spot §813, repressed 24h after UV-C stress, was identified as a voltage-dependent anion channel. It is involved in hypersensitive response (HR) as well as in controlling flux of signalling metabolites and ions across the membranes during plant defense responses, suggesting an active role in mantaining cell homeostasis and signalling modulation.

Carbonic anhydrase was found to be repressed in spot §840. This zinc metalloenzyme catalyzes the reversible hydration of CO_2 into HCO_3^- and represents a major protein constituent of the C3 higher plant chloroplasts, where it plays a role in photosynthetic carbon assimilation as well as in response to biotic and abiotic stresses.

We found a down regulation of a ROS scavenging enzyme: the quinone oxidoreductase (QO - spot §591). Many polyphenols, like flavonoids (including genistein, kaempferol, morin and quercetin), have been reported to induce QO, which is thus used in human as a biomarker of phase II metabolic activity in carcinogen elimination (Moon et al. 2006). Unexpectedly, the increase of polyphenols (up to 4 fold) would suggest a different QO behaviour. Notwithstanding, QO down regulation at 24h cannot exclude a positive regulation in earlier steps of UV-C responses.

Other functions

The spot §570, induced at 24h, was identified as an RNA-binding protein with pentatricopeptide repeats and ribonuclease activity (Kun et al. 2011). Blast analysis revealed a high similarity with

CSP41a/CSP41b, a protein having a role in chloroplast ribosomal RNA metabolism, most likely acting in the final steps of 23S rRNA maturation (Bollenbach et al. 2009). No information on its role in abiotic stress are available to date.

The level of fructan 1-exohydrolase (1-FEH, spot §147), involved in inulin degradation, was induced by UV-C. In accordance to our results, it has been demonstrated that 1-FEH is highly expressed in *Cichorium intybus*, after stress conditions (cold-stored roots) (Michiels et al. 2004). Inulin is a polysaccharide used by many plants as a means of storing energy and thus the 1-FEH overexpression following stress could be a quick way to mobilise energy on demand. Inulin is of particular interest in human nutrition, as alternative for low-calory sweetener, dietary fibre or as a fat substitute, as well as stimulator of *Bifidobacteria* and *Lactobacilli* in the colon (Michiels et al. 2004; Van den Ende et al. 2004; Yamamori et al. 2002; Ramnani et al. 2010) and in the prevention of osteoporosis, colon and breast cancer (Michiels et al. 2004). Since globe artichoke is able to produce high quantities of inulin with high degree of polymerization (Ronkart et al. 2007), silencing of 1-FEH could, in a breeding perspective, help to further increase inulin yield in large scale production.

Conclusions

In this study, we analysed the globe artichoke PEG enriched proteome 24 hours after UV-C stimulus, when phenolics reach their higher levels. Most of the detected modulated proteins were located in the chloroplasts and mainly involved in primary metabolisms, while a number of enzymes related to accessory metabolic pathways, protein targeting and regulation of transcription were highlighted. UV-C stress, by troubling leaf homeostasis, led to an enhanced accumulation of toxic compounds, which, driving out energy from plant cell primary metabolisms, might be counterbalanced by the production of antioxidant protective molecules.

In general, on the statement that "the whole is more than the sum of its parts" (Aristotle, Metaphysics - 1045a10), a deeper investigation of the protein networks acting in the UV response is still required as it will permit to establish a comprehensive knowledge about the mechanisms governing plant responses against abiotic stress: time-course experiments following stimulus, as well as different proteome pre-fractionations (e.g. Proteominer™ or analogous tools) will led to an increasing number of visible occurring emergent proteins/phenomena.
The highlighted gene functions will be relevant to establish breeding programs aimed at enhancing plant tolerance to stress, and exploiting genes for biotechnological purposes.

Figure captions:

Fig 1 – Experimental design: A) UV-C stress procedure, B) PEG fractioning, C) representative PEG-enriched proteome 2-DE gel.

Fig 2 – UV-C modulated proteins on the globe artichoke leaf 2-DE mapMw: molecular weight. pI: isoelectric point; NL: non-linear gradient.

Fig 3 - Categorisation of the 38 UV-C responsive proteins using Gene Ontology. Pie charts show molecular function, cellular component, and biological process protein distribution.

Fig 4 -; A) snapshot on the photosynthesis "Light reactions"; B) snapshot on the Calvin cycle. The numbers indicated in 4A and 4B refer to the spots that were analysed from the gel represented in Fig. 2. The black squares indicates the fold up-regulation, while the white squares the fold down-regulation of the proteins; their relative expression levels are showed using a gray-scale of intensity.

Supplementary material 1 – Bar diagram of the UV-C modulated proteins with fold change and standard error.

Supplementary material 2 – Protein identification from the globe artichoke PEG enriched proteome 24 hours after UV-C irradiation with peptides.

Acknowledgements

This research has been enabled by a grant from “Progetto Lagrange-Fondazione CRT”. The research was performed in the context of the project iTECHPLAT Intervention, co-financed by the EU on the Measure 3.4 of the Regione Piemonte docup 2000/2006, supported and implemented by Polo di Innovazione Provinciale of the Province of Turin 2009. Special thanks are due to Franco Fedeli for his training on HPLC analysis.

References

Acquadro A, Falvo S, Mila S, Albo A, Comino C, Moglia A, Lanteri S. (2009) Proteomics in globe artichoke: Protein extraction and sample complexity reduction by PEG fractionation. Electrophoresis 30, (9): 1594-1602.

Ahsan N, Lee D, Alam I, Kim P, Lee J, Ahn Y, Kwak S, Lee I, Bahk J, Kang K, Renaut J, Komats US, Lee B. (2008) Comparative proteomic study of arsenic-induced differentially expressed proteins in rice roots reveals glutathione plays a central role during As stress. Proteomics 3561-3576.

Albo A, Mila S, Digilio G, Motto M, Aime S, Corpillo D. (2007) Proteomic analysis of a genetically modified maize flour carrying Cry1Ab gene and comparison to the corresponding wild-type. Maydica 443-455.

Bian F, Zheng C, Qu F, Gong X and You C. (2010) Proteomic analysis of somatic embryogenesis in *Cyclamen persicum* Mill. Plant Molecular Biology Reporter, 28, (1): 22-31.

Bollenbach, T.; Sharwood, R.; Gutierrez, R.; Lerbs-Mache, S.; Stern, D., (2009) The RNA-binding proteins CSP41a and CSP41b may regulate transcription and translation of chloroplast-encoded RNAs in *Arabidopsis.* Plant Mol. Biol. 541-552.

Braam J, Davis R. (1990) Rain-induced, wind-induced, and touch-induced expression of Calmodulin and Calmodulin-related genes in *Arabidopsis*. Cell, 357-364.

Braam J. (1992) Regulation of expression of Calmodulin and Calmodulin-related genes by environmental stimuli in plants. Cell Calcium 457-463.

Bradford M. (1976) A rapid and sensitive method for quantitation of microgram quantities of protein utilizing the principle of protein-dye-binding. Anal. Biochem 72:248-254.

Casati P, Zhang X, Burlingame AL and Walbot V. (2005) Analysis of leaf proteome after UV-B irradiation in maize lines differing in sensitivity. Molecular & Cellular Proteomics; 4: 1673–1685.

Cho S, Kim J, Park J, Eom T, Kim W. (2006) Constitutive expression of abiotic stress-inducible hot pepper CaXTH3, which encodes a xyloglucan endotransglucosylase/hydrolase homolog, improves drought and salt tolerance in transgenic *Arabidopsis* plants. FEBS Letters 3136-3144.

Conesa A, Gotz S, Garcia-Gomez J, Terol J, Talon M, Robles M. (2005) Blast2GO: a universal tool for annotation, visualization and analysis in functional genomics research. Bioinformatics 21, (18): 3674-3676.

Coohill T. (1999) Conventional UV-visible sources. Photochem. Photobiol 15S-15S.

Damerval C, De Vienne D, Zivy MHT. (1986) Technical improvements in two-dimensional electrophoresis increase the level of genetic variation detected in wheat-seedling proteins. Electrophoresis 7:52–54.

Ding C, You J, Liu Z, Rehmani MIA,Wang S, Li G, Wang Q and Ding Y. (2011) Proteomic analysis of low nitrogen stress-responsive proteins in roots of rice. Plant Molecular Biology Reporter, 10.1007/s11105-010-0268-z.

Dong M, Zhang X, Zhuang Z, Zou J, Ye N, Xu D, Mou S, Liang C and Wang W. (2011) Characterization of the LhcSR gene under light and temperature stress in the green alga *Ulva linza*. Plant Molecular Biology Reporter, 10.1007/s11105-011-0311-8.

Du HM, Liang Y; Pei KQ, Ma K. (2011) UV radiation-responsive proteins in rice leaves: a proteomic analysis Plant and Cell Physiology 52, (2): 306-316.

Feng L, Wang K, Li Y, Tan Y, Kong J, Li H, Li Y, Zhu Y. (2007) Overexpression of SBPase enhances photosynthesis against high temperature stress in transgenic rice plants. Plant Cell Rep. 1635-1646.

Iliev E, Xu W, Polisensky D, Oh M, Torisky R, Clouse S, Braam J. (2002) Transcriptional and posttranscriptional regulation of *Arabidopsis* TCH4 expression by diverse stimuli. Roles of cis regions and brassinosteroids. Plant Physiol. 770-783.

Jellouli N, Jouira HB, Daldoul S, Chenennaoui S, Ghorbel A, Salem AB and Gargouri A. (2010) Proteomic and transcriptomic analysis of grapevine pr10 expression during salt stress and functional characterization in yeast. Plant Molecular Biology Reporter, 28,(1): 1-8.

Kaspar S, Matros A, and Mock HP. (2010) Proteome and flavonoid analysis reveals distinct responses of epidermal tissue and whole leaves upon UV−B Radiation of barley (*Hordeum vulgare* L.) seedlings. Journal of Proteome Research 9, (5): 2402-2411.

Kasprzewska A. (2003) Plant chitinases - Regulation and function. Cell. Mol. Biol. Lett. 809-824.

Kun W, Feng G, Renshan Z, Shaoqing L and Yingguo Z. (2011) Expression, Purification, and Secondary Structure Prediction of Pentatricopeptide Repeat Protein RF1A from Rice). Plant Molecular Biology Reporter, 10.1007/s11105-010-0260-7.

Kuun K, Okole B, Bornman L. (2001) Protection of phenylpropanoid metabolism by prior heat treatment in Lycopersicon esculentum exposed *to Ralstonia solanacearum*. Plant Physiol. and Biochem. 871-880.

Lefebvre S, Lawson T, Zakhleniuk O, Lloyd J, Raines C. (2005) Increased sedoheptulose-1,7-bisphosphatase activity in transgenic tobacco plants stimulates photosynthesis and growth from an early stage in development. Plant Physiol 451-460.

Li D, Staehelin C, Wang W and Peng S. (2010) Molecular cloning and characterization of a chitinase-homologous gene from *Mikania micrantha* infected by *Cuscuta campestris*. Plant Molecular Biology Reporter, 28, (1): 90-101.

Michiels A, Van Laere A, Van den Ende W, Tucker M. (2004) Expression analysis of a chicory fructan 1-exohydrolase gene reveals complex regulation by cold. J. Exp. Bot. 1325-1333.

Miyagawa Y, Tamoi M, Shigeoka S. (2001) Overexpression of a cyanobacterial fructose-1,6-/sedoheptulose-1,7-bisphosphatase in tobacco enhances photosynthesis and growth. Nat. Biotechnol. 965-969.

Moglia A, Lanteri S, Comino C, Acquadro A, de Vos R, Beekwilder J. (2008) Stress-induced biosynthesis of dicaffeoylquinic acids in globe artichoke. J. Agric. Food Chem 56, (18): 8641-8649.

Moon Y, Wang X, Morris M. (2006) Dietary flavonoids: Effects on xenobiotic and carcinogen metabolism. Toxicol. in Vitro 187-210.

Petit A, Baillieul F, Vaillant-Gaveau N, Jacquens L, Conreux A, Jeandet P, Clement C, Fontaine F. (2009) Low responsiveness of grapevine flowers and berries at fruit set to UV-C irradiation. J. Exp. Bot. 1155-1162.

Polisensky D, Braam J. (1996) Cold-shock regulation of the arabidopsis TCH genes and the effects of modulating intracellular calcium levels. Plant Physiol. 1271-1279.

Qian L, Wenyu Y, Xiaoping Y, Songlin R and Haifeng C, Huasheng M and Zihong Y. (2011) A preliminary study on proteome variations associated with gall formation in *Zizania latifolia Trucs*). Plant Molecular Biology Reporter, 29, (2): 360-368.

Ramnani PGE, Bingham M, van Bruggen P, Tuohy KM, Gibson GR. (2010) Prebiotic effect of fruit and vegetable shots containing Jerusalem artichoke inulin: a human intervention study. Br J Nutr. 1: 1-8.

Regalado A, Pinheiro C, Vidal S, Chaves I, Ricardo C, Rodrigues-Pousada C. (2000) The *Lupinus albus* class-III chitinase gene, IF3, is constitutively expressed in vegetative organs and developing seeds. Planta 543-550.

Righetti P, Boschetti E. (2007) Sherlock Holmes and the proteome - a detective story. Febs J. 274, (4): 897-905.

Ronkart S, Blecker C, Fourmanoir H, Fougnies C, Deroanne C, Van Herck J, Paquot M. (2007) Isolation and identification of inulooligosaccharides resulting from inulin hydrolysis. Anal. Chim. Acta 81-87.

Scaglione D, Acquadro A, Portis E, Taylor CA, Lanteri S, Knapp SJ. (2009) Ontology and diversity of transcript-associated microsatellites mined from a globe artichoke EST database. BMC Genomics 10, (1): 454.

Shevchenko A, Tomas H, Havlis J, Olsen J, Mann M. (2006) In-gel digestion for mass spectrometric characterization of proteins and proteomes. Nature Protocols 2856-2860.

Singh A, Sarkar A, Singh S, Agrawal SB. (2010) Investigation of supplemental ultraviolet-B-induced changes in antioxidative defense system and leaf proteome in radish (*Raphanus*

sativus L. cv Truthful): an insight to plant response under high oxidative stress. Protoplasma: 1-9.

Stapletons A. (1992) Ultraviolet-radiation and plants - burninig questions. Plant Cell 1353-1358.

Timperio A, Egidi M, Zolla L. (2008) Proteomics applied on plant abiotic stresses: Role of heat shock proteins (HSP). J. Proteomics 391-411.

Van den Ende W, De Coninck B, Van Laere A. (2004) Plant fructan exohydrolases: a role in signaling and defense? Trends in Plant Sci. 523-528.

Wang M, Simon J, Aviles I, He K, Zheng Q, Tadmor Y. (2003) Analysis of antioxidative phenolic compounds in artichoke (*Cynara scolymus* L.). J. Agric. Food Chem 51, (3): 601-608.

Wang W, Vinocur B, Shoseyov O, Altman A. (2004) Role of plant heat-shock proteins and molecular chaperones in the abiotic stress response. Trends in Plant Sci. 244-252.

Winkel B. (2004) Metabolic channeling in plants. Annu. Rev. Plant Biol. 85-107.

Xu C, Sullivan JH, Garrett WM, Caperna TJ and Natarajan S. (2008) Impact of solar ultraviolet-B on the proteome in soybean lines differing in flavonoid contents. Phytochemistry 69, (1): 38-48.

Yamamori A, Onodera S, Kikuchi M, Shiomi N. (2002) Two novel oligosaccharides formed by 1(F)-fructosyltransferase purified from roots of asparagus (*Asparagus officinalis* L.). Biosci. Biotechnol., Biochem. 1419-1422.

Yang Q, Wang Y, Zhang J, Shi W, Qian C, Peng X. (2007) Identification of aluminum-responsive proteins in rice roots by a proteomic approach: Cysteine synthase as a key player in Al response. Proteomics 737-749.

Zhang J, Sun L, Liu L, Lian J, An S, Wang X, Zhang J, Jin J, Li S and Xi J. (2010) Proteomic analysis of interactions between the generalist herbivore *Spodoptera exigua* (Lepidoptera: Noctuidae) and *Arabidopsis thaliana.* Plant Molecular Biology Reporter, 28, (2): 324-333.

New Figure 1

Click here to download Figure: NEWFIG1.ppt

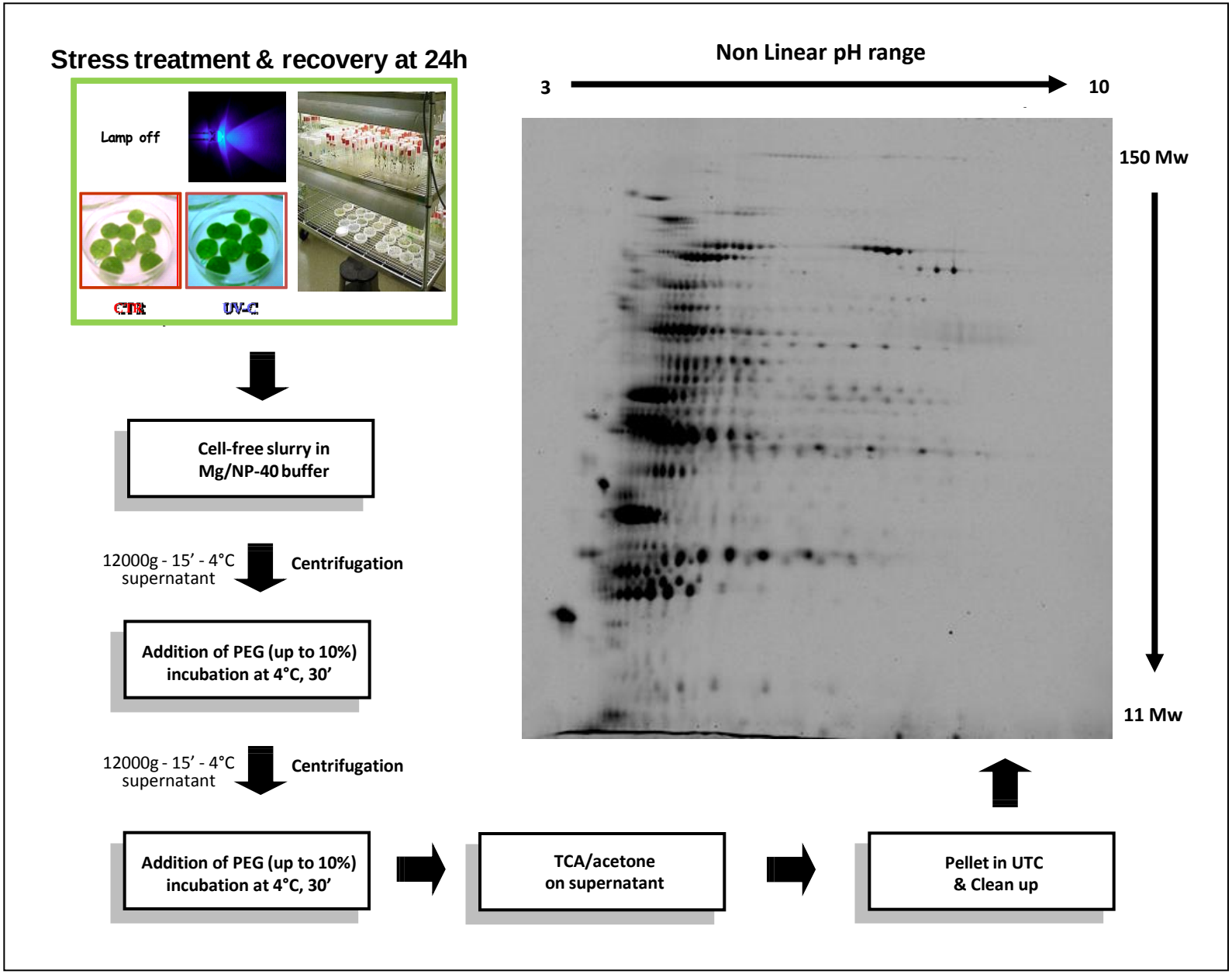

New Figure 2

FIGURE 3

Click here to download Figure: NEWFIG2.ppt

24h after UV-C STIMULUS

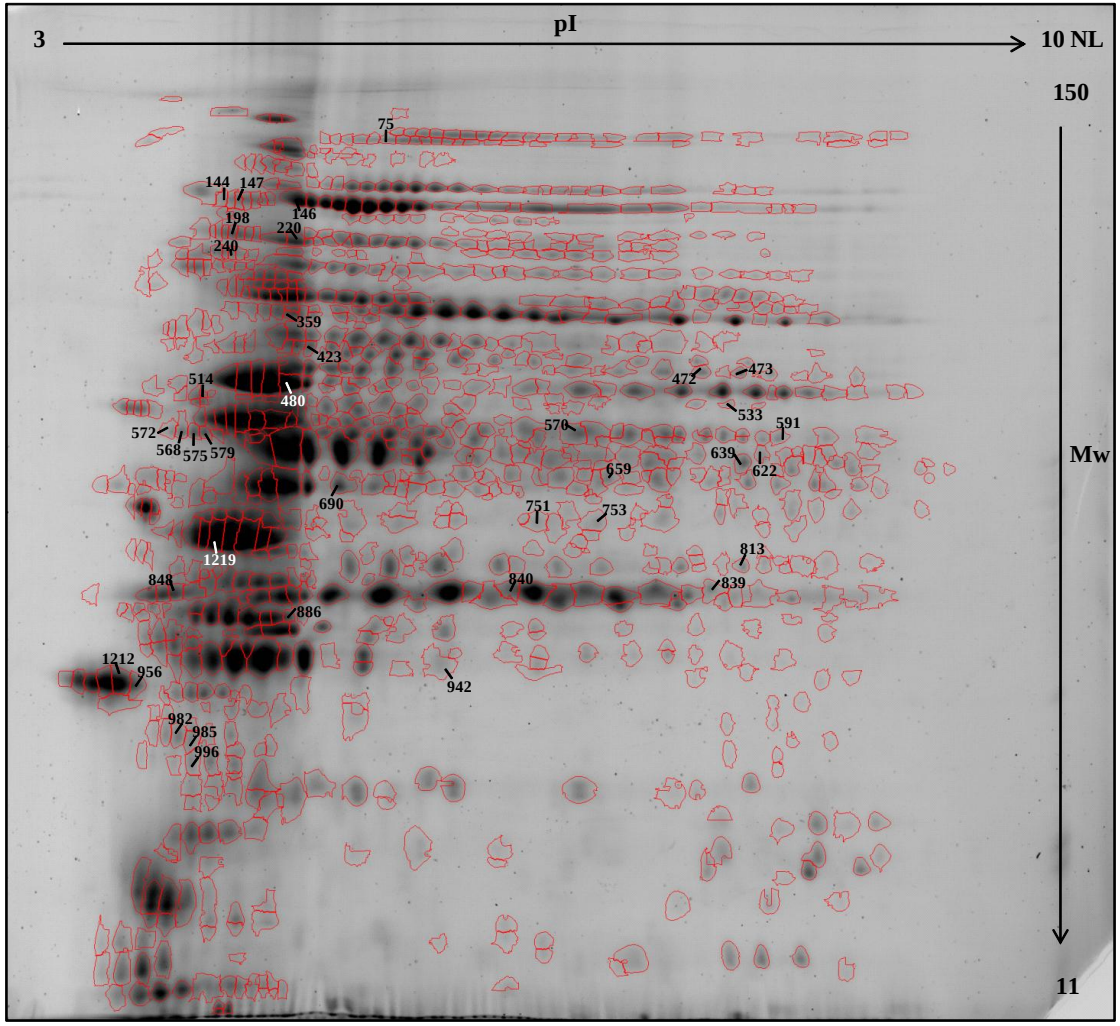

38 spots: 16 UP, 22 DOWN

New Figure 3

Click here to download Figure: NEWFIG3.ppt

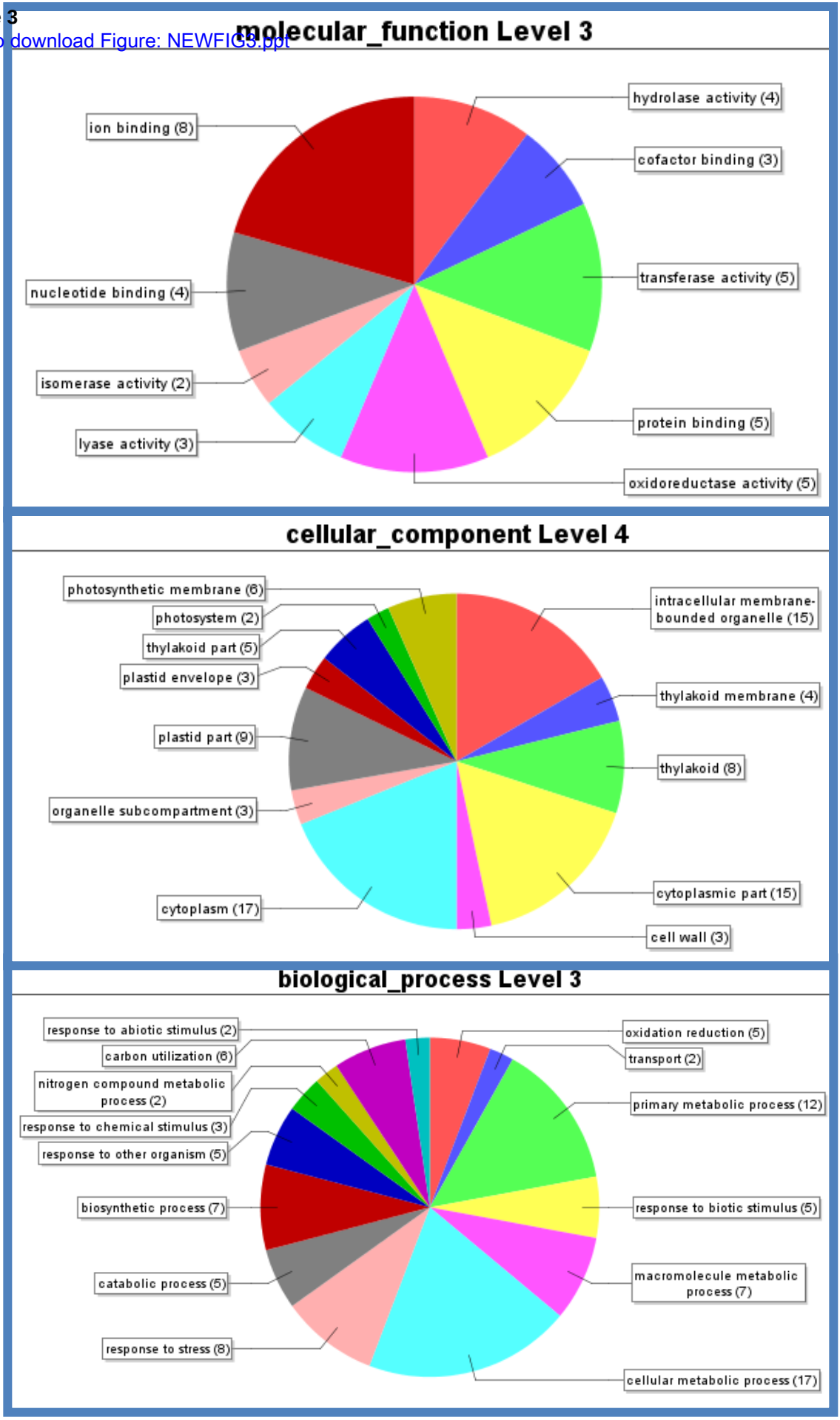

New Figure 4

Click here to download Figure: NEWFIG4_a_b.ppt

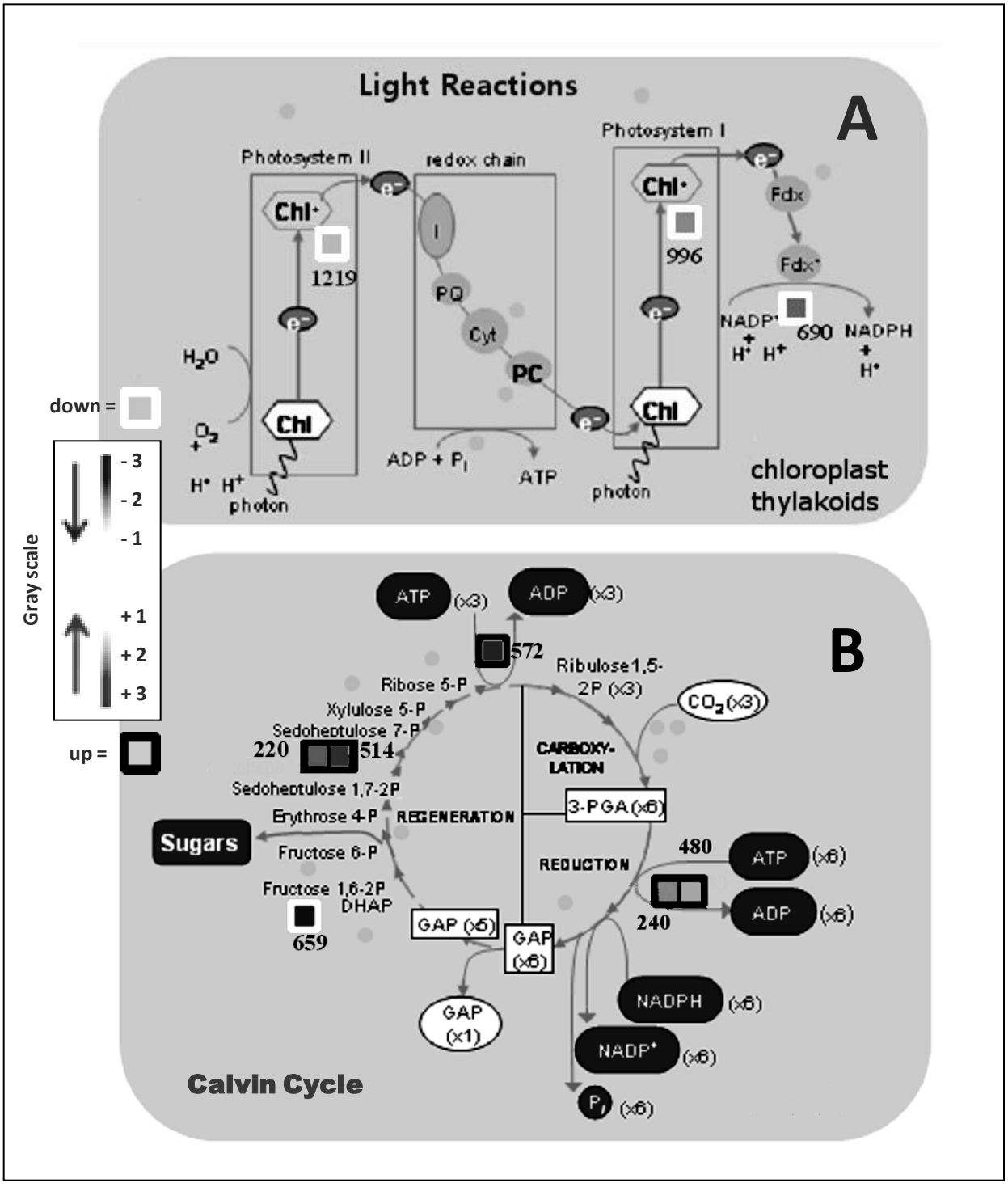

Table 1

Click here to download Table: Table1_REVISED.doc

Tables

Table 1 - Protein identification from the globe artichoke PEG enriched proteome 24 hours after UV-C irradiation.

[1]Differentially expressed protein spots were selected according to: (i) a p-value cutoff of 0.05; (ii) a fold change threshold of 1.50; and (iii) spot presence in the 80% of the maps. [2]AGI code: are the unique locus identifiers from *Arabidopsis* orthologs. [3]Theoretical molecular weight and iso-electric points desumed from *Arabidopsis* putative orthologs (www.arabidopsis.org).

Spot ID[1]	Protein annotation	AGI code[2]	Score	Coverage	E.C. number	MW[3] (KDa) obs./theor.	pI[3] obs./theor.	Fold change	Vol% (UV)	Sd (UV)	Vol% (wt)	Sd (w)t	Anova
Up-regulated													
579	Cysteine synthase	AT2G43750	352	30%	2.5.1.47	38,0/41.6	4.5/8.2	7,62	0.059167	0.044361	0.009704	0.003978	0.035
568	FBP aldolase	AT3G59480	315	34%	2.7.1.4	38,0/35,0	4.5/4.9	5,31	0.059167	0.013438	0.010274	0.002525	0.001
848	Acidic endochitinase	AT5G24090	74	3%	3.2.1.14	30,0/33,1	4.2/9.3	5,18	0.055591	0.039473	0.013406	0.010578	0.043
572	Phosphoribulose kinase	AT1G32060	59	8%	2.7.1.19	41,0/44,3	4.2/5.9	4,70	0.033318	0.010023	0.00887	0.004556	0.002
570	RNA binding protein	AT1G09340	96	17%	-	40,0/42,6	6.7/8.4	3,03	0.059805	0.020087	0.024703	0.017603	0.018
144	Hsp70	AT4G24280	431	25%	-	78,0/76,5	4.0/4.8	2,83	0.03891	0.018205	0.01716	0.007217	0.032
514	Sedoheptulose-bisphosphatase	AT3G55800	646	71%	3.1.3.37	43,0/42,4	4.2/6.5	2,73	0.014275	0.005897	0.006542	0.00501	0.045
147	fructan 1-exohydrolase	AT5G11920	61	35%	3.2.1.80	78,0/62,1	4.5/4.7	2,13	0.031214	0.009962	0.018283	0.002689	0.031
639	ADH	AT5G43940	62	11%	1.1.1.1	39,0/40,6	7.2/6.9	1,97	0.048809	0.01278	0.023743	0.005852	0.007
220	Sedoheptulose-bisphosphatase	AT3G55800	358	63%	3.1.3.37	65,0/42,4	5.2/6.5	1,91	0.076151	0.006623	0.049747	0.017325	0.035
240	PGKs	AT1G56190	93	15%	2.7.2.3	60,0/49,9	4.5/8.6	1,66	0.013543	0.004136	0.008907	0.000836	0.033
480	PGKs	AT1G56190	1294	81%	2.7.2.3	45,0/49,9	5.2/8.6	1,44	0.207481	0.029503	0.142868	0.041214	0.026
Down-regulated													
1219	OEC 33 kDa photosystem II	AT3G50820	164	28%	-	34,0/35,0	5.2/5.9	-1,22	0.297071	0.042314	0.356695	0.032699	0.032
473	ADH	AT5G43940	142	18%	1.1.1.1	45,0/40,7	7.2/6.9	-1,52	0.016067	0.005061	0.022106	0.005628	0.048
996	OEC 33 kDa photosystem II protein	AT5G66570	114	26%	-	25,0/35,1	4.5/5.2	-1,53	0.028339	0.004207	0.041385	0.008146	0.014
472	ADH	AT5G43940	113	20%	1.1.1.1	45,0/40,7	7.0/6.9	-1,62	0.021594	0.002757	0.031237	0.007929	0.048
840	Carbonic anhydrase	AT3G01500	96	24%	4.2.1.1	30,0/29,5	6.5/5.4	-1,71	0.073575	0.0198	0.110915	0.025391	0.048
690	Ferredoxin-NADP+ oxido-reductase	AT5G66190	125	23%	1.18.1.2	35,0/40,3	6.2/8.3	-1,75	0.050456	0.025717	0.084652	0.016983	0.032
751	Xyloglucan endotransglucosylase	AT4G37800	143	12%	3.2.1.0	32,0/33,7	6.5/7.4	-1,96	0.01916	0.006132	0.035653	0.011882	0.022
591	Quinone oxidoreductase	AT4G13010	266	41%	-	40,0/34,4	8.5/9.4	-2,02	0.014518	0.012173	0.028249	0.004899	0.040
198	GMC oxidoreductase	AT5G51930	68	12%	-	68,0/64,1	4.3/6.8	-2,04	0.017506	0.007781	0.035709	0.004768	0.003
886	Cytosolic triose phosphate isomerase	AT3G55440	537	48%	5.3.1.1	27,0/27,2	5.2/5.2	-2,25	0.024508	0.01034	0.058146	0.008306	0.003
813	Voltage-dependent anion channel	AT3G01280	112	9%	-	30,0/29,4	8.5/9.2	-2,35	0.0113	0.007616	0.025958	0.00752	0.015
359	1-deoxy-D-xylulose 5-phosphate	AT5G62790	171	10%	1.1.1.267	50,0/51,9	5.3/7.0	-3,25	0.015669	0.007973	0.05032	0.006826	0.0001
659	FBP aldolase	AT3G59480	93	10%	4.1.2.13	38,0/35,0	6.2/5.0	-3,67	0.016137	0.011907	0.058872	0.030762	0.021

Supplementary Material 1

Suppl. Data 2

Click here to download Supplementary Material: Suppldata_1.ppt

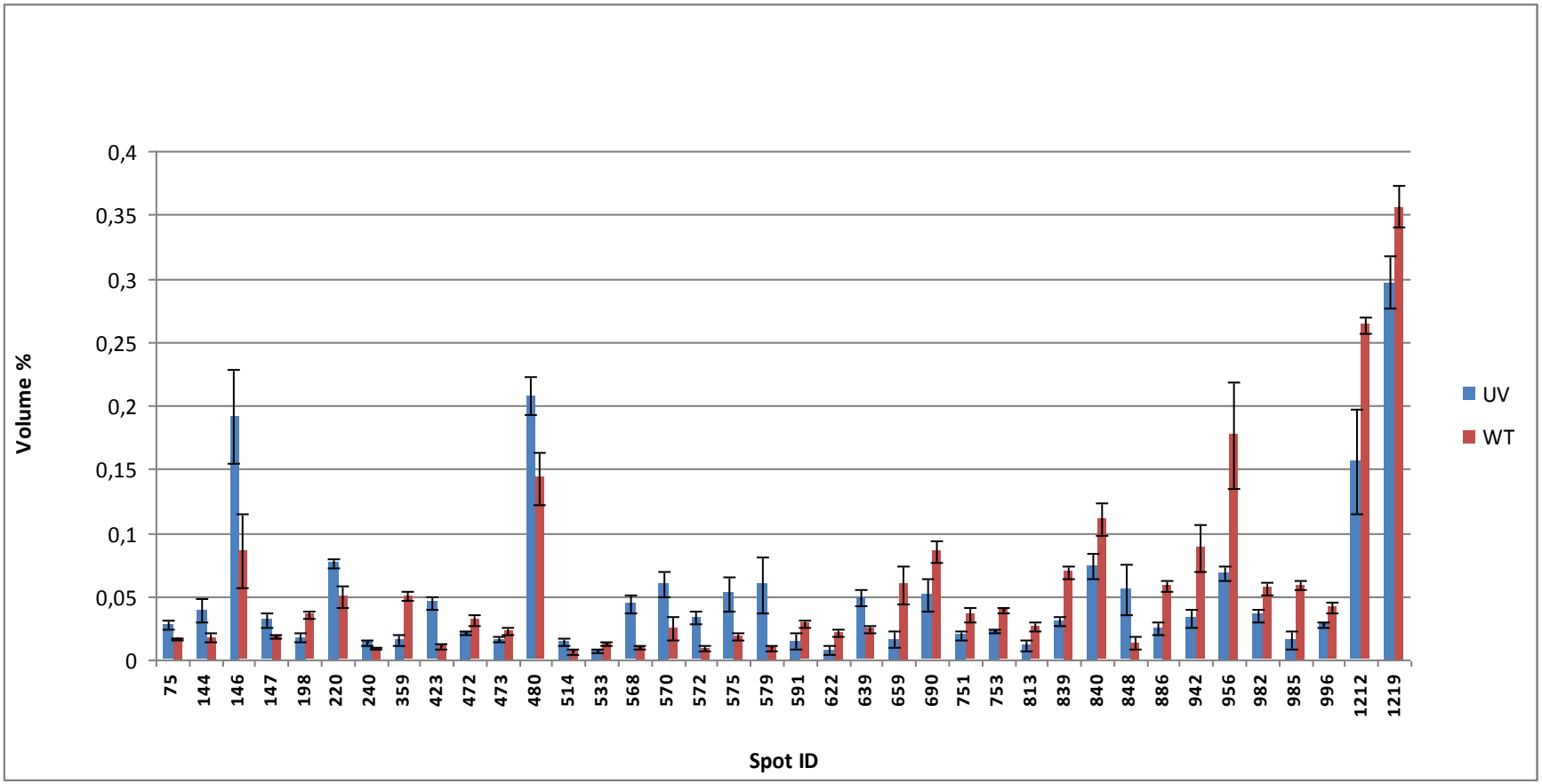

Supplementary Material 2

Click here to download Supplementary Material: Suppldata_2_REV.doc

Suplpemental Data 1

spot ID	PRI id	Compositae accession	Protein description	Mascot Score	Peptide sequence	Peptide charge state	Peptide score	Queries matched	Coverage
75	n.i	n.i.	n.i.	n.i.	n.i.		n.i.	n.i.	n.i.
144	PRid000025896	LacSat_TC22779	hsp70	431	IAGLEVLR	2	59	15	25%
					LDCPAIGK	2	45		
					HIDTTLTR	2	34		
					KDEGIDLLK	2	39		
					TTPSVVAYTK	2	31		
					EAISGGSTQTIK	2	58		
					DLDEVILVGGSTR	2	52		
					NQADSVVYQTEK	2	81		
					FEELCSDLLDR	2	67		
					QFAAEEISAQVLR	2	104		
					AVVTVPAYFNDSQR	2	29		
					QAVVNPENTFFSVK	2	71		
					IINEPTAASLAYGFER	2	114		
					VVGIDLGTTNSAVGAMEGGKPVIVTNAEGQR	3	65		
					VVGIDLGTTNSAVGAMEGGKPVIVTNAEGQR **Oxidation (M)**	3	108		
	PRid000001794	Artch_CL472Contig1		424	IAGLEVLR	2	59	18	36%
					LDCPAIGK	2	45		
					APVENSLR	2	51		
					HIDTTLTR	2	34		
					IPAVQEVIK x 2	2	47		
					KDEGIDLLK	2	39		
					VVDWLAASFK	2	82		
					EAISGGSTQTIK	2	58		
					DLDEVILVGGSTR	2	52		
					NQADSVVYQTEK	2	81		
					FEELCSDLLDR	2	67		
					QFAAEEISAQVLR	2	104		

					GPEGDVIDADFTDSK	2	32		
					AVVTVPAYFNDSQR	2	29		
					FDIDANGILSVTAIDK	2	99		
					IINEPTAASLAYGFER	2	114		
					QDITITGASTLPNDEVQR	3	44		
					KQDITITGASTLPNDEVQR	3	46		
146	n.i.	n.i.	n.i.	n.i.	n.i.		n.i.	n.i.	n.i.
147	PRid000016119	Artch_CCPX2318.b1_K03.ab1	Fructan 1-exohydrolase	61	GWAGLQSFPR	2	60	4	35%
					VLWGWIPESDSQEDDIEK	2	26		
					KLDSACPVYEIQGITASQADVTVSFK	3	31		
					AGFEGHDWYTIGTYSPVSENFLPQNGLR **Deamidated (NQ)**	3	38		
198	PRid000016744	Artch_CCPX4229.b1_I01.ab1	GMC oxidoreductase	68	VVVEQPLVGQYMADNPLNGFFIPALVPVER	3	55	2	12%
					VVVEQPLVGQYMADNPLNGFFIPALVPVER **Deamidated (NQ)**	3	51		
220	PRid000002237	Artch_CL2128Contig1	sedoheptulose-bisphosphatase	358	TTYVLAIK	2	22	9	63%
					FEETLYGSSR	2	78		
					GVFTNVISPTTK	2	66		
					YTGGMVPDVNQIIVK **Oxidation (M)**	2	23		
					GFPGTHEFLLLDEGK	3	27		
					VIVNLDDRTQVAYGSK	3	52		
					LTGVTGGDQVAAAMGIYGPR	2	144		
					ATFDNPEYDKLINYYVK	3	59		
					LLFEVAPLGLLIENAGGYSSDGTK x 2	3	114		
240	PRid000005257	Artch_CL962Contig1	PGK	93	GVTTIIGGGDSVAAVEK	2	56	3	15%
					VGVADVMSHISTGGGASLELLEGK **Oxidation (M)**	3	47		
					AQGLSVGSSLVEEDKLDLATTLLAK	3	56		
359	PRid000080962	HelAn_TC49682	1-deoxy-D-xylulose 5-phosphate	171	IILTASGGAFR	2	51	4	10%
			reductase		ITVDSATLFNK	2	66		
					AGGTMTGVLSAANEK	2	104		
					LPILYTLSWPDR	2	67		
	PRid000056525	LacSer_TC7585		159	ITVDSATLFNK	2	66	3	19%
					AGGTMTGVLSAANEK	2	104		
					IPILYTLSWPDR	2	67		
	PRid000009840	Artch_CCPU9555.b1_F14.ab1		153	**YPSMDLAYSAGR**	2	61	3	24%

					AGGTMTGVLSAANEK	2	104		
					LPILYTLSWPDR	2	67		
423	PRid000004018	Artch_CL2520Contig1	SAM synthase	346	NGTCAWLRPDGK **Deamidated (NQ)**	2	33	8	34%
					FVIGGPHGDAGLTGR x 2	2	93		
					TNMVMVFGEITTK	2	119		
					EIGFVSDDVGLDADNCK	2	105		
					TQVTVEYHNDNGAMVPLR x 2	2	82		
					LCDQISDAVLDACLAQDPDSK	3	68		
					VLVNIEQQSPDIAQGVHGHLTK	3	43		
					AIVQVSYAIGVPEPLSVFVDTYGTGK	3	52		
	PRid000003348	Artch_CL61Contig1	NADP+ isocitrate dehydrogenase	226	**NILNGTVFR Deamidated (NQ)**	2	28	8	21%
					DLALIIHGSK	2	54		
					YYDLGLLNR	2	67		
					LIDDMVAYALK	2	76		
					LIFPFVDLDIK	2	53		
					SKFEAAGIWYEHR	3	53		
					GGETSTNSIASIFAWTR	2	105		
					DATDDKVTIESAEATLK	3	47		
472	PRid000022848	LacSat_TC19731	ADH	113	IDPQAPLEK	2	22	4	20%
			(glutathione-dependent		VQILFTALCHTDAYTWSGK	3	27		
			formaldehyde dehydrogenase)		AAVAYEANKPLVIEDVEVAPPQAGEVR	3	34		
					GWGTSVIVGVAASGQEISTRPFQLVTGR	3	113		
473	PRid000022848	LacSat_TC19731	ADH	142	TQVPQLVDK	2	21	4	18%
			(glutathione-dependent		VCLLGCGVPTGLGAVWNTAK	2	47		
			formaldehyde dehydrogenase)		VQILFTALCHTDAYTWSGK	2	81		
					GWGTSVIVGVAASGQEISTRPFQLVTGR	3	81		
	PRid000002288	Artch_CL2320Contig1		95	VCLLGCGVPTGLGAVWNTAK	2	47	3	24%
					VQILFTALCHTDAYTWSGK	2	81		
					VEAGSNVAIFGLGTVGLAVAEGAK	3	28		
	PRid000014201	Artch_CCPW7546.b2_C16.ab1		66	TQVPQLVDK	2	21	4	27%
					QFGVTEFVNPK	2	58		
					VCLLGCGVPTGLGAVWNTAK	2	47		
					VEAGSNVAIFGLGTVGLAVAEGAK	3	28		

480	PRid000005257	Artch_CL962Contig1	Phosphoglycerate kinase	1294	KLAELSGK	2	41	26	81%
					FAPDANSK	2	37		
					YLITNGAK **Deamidated (NQ)**	2	37		
					NDPAFAEK	2	44		
					AHASTEGVTK	2	36		
					YSLAPLVSR	2	38		
					FAVGTEAIAK	2	66		
					IGVIESLLEK	2	78		
					RPFAAIVGGSK	2	61		
					SVGDLSPAQLK x 3	2	52		
					TFNDALETTK	2	58		
					LSELIGIQVVK	2	88		
					VILSSHLGRPK	2	39		
					ADDCVGPEVEK	2	64		
					KSVGDLSPAQLK	2	68		
					ELDYLDGAVSNPK	2	77		
					FLRPSVAGFLLQK x 2	2	72		
					GVSLLLPTDVVVADK x 2	2	39		
					GVTTIIGGGDSVAAVEK x 2	2	102		
					TLPGVDALDEAVVAVSA x 2	2	63		
					LVASLAEGGVLLLENVR x 7	2	88		
					CDILLLGGGMIFTFYK x 4 **Oxidation (M)**	2	110		
					LASIADLYVNDAFGTAHR x 2	2	112		
					ADLNVPLDDNQNITDDTR x 3	2	62		
					VGVADVMSHISTGGGASLELLEGK x 4 **Oxidation (M)**	3	80		
					AQGLSVGSSLVEEDKLDLATTLLAK x 5	3	112		
514	PRid000002237	Artch_CL2128Contig1	Sedoheptulose-bisphosphatase	646	TQVAYGSK	2	38	19	71%
					TTYVLAIK	2	36		
					LINYYVK	2	43		
					MFSPGNLR x 2	2	38		
					MFSPGNLR x 2 **Oxidation (M)**	2	32		
					VIVNLDDR	2	47		
					ETTEISEGK	2	42		

					FEETLYGSSR	2	63		
					ATFDNPEYDK	2	52		
					GVFTNVISPTTK	2	70		
					EKGVFTNVISPTTK	2	44		
					YTGGMVPDVNQIIVK x 3	3	44		
					YTGGMVPDVNQIIVK x 2 **Oxidation (M)**	2	64		
					GFPGTHEFLLLDEGK x 2	2	82		
					VIVNLDDRTQVAYGSK x 4	2	74		
					LTGVTGGDQVAAAMGIYGPR x 2	2	144		
					LTGVTGGDQVAAAMGIYGPR **Oxidation (M)**	2	110		
					ATFDNPEYDKLINYYVK x 2	3	46		
					LLFEVAPLGLLIENAGGYSSDGTK	2	133		
533	n.i.	n.i.	n.i.	n.i.	n.i.		n.i.	n.i.	n.i.
568	PRid000003765	Artch_CL1553Contig1	FBP aldolase	315	TALAFVTLK	2	53	9	34%
					LLLVTLGDK	2	62		
					NFHGTVGAFAVK	2	45		
					LPLWPSPEEAR x 2	2	31		
					YACACGAITTTK	2	68		
					IVDDHSVLEDEGK	2	79		
					VSDNELEFLTGCEK	2	78		
					AVDTTGAGDSFVGALLTK	2	126		
					GAIPALPTVSEVQGFIK	2	76		
570	PRid000002014	Artch_CL1282Contig1	RNA binding protein	96	SLVLS	1	32	5	17%
					FIGIFLSR	2	41		
					AGGFPEPEIIHYNPK	3	23		
					APITQPLPGESDEAYNAFK	2	83		
					AGRPIPIPNSGIQVTQLGHVK	3	42		
572	PRid000000849	Artch_CL3231Contig1	Phosphoribulose kinase	59	LTSVFGGAAEPPR	2	59	2	8%
					QYADAVIEVLPTQLIPGDNEGK	3	33		
	PRid000017616	Artch_CCPX6419.b1_E22.ab1		57	YAAISQDNGLVPIVEPEILLDGEHGIDR	3	57	1	14%
	PRid000120890	HelAn_GE514903		53	VVVYPVSEEYILEK	2	53	1	10%
	PRid000102267	HelAn_BQ916125		53	VVVYPVSEQYILEK	2	53	1	13%
575	PRid000020053	LacSat_TC16936	Fructokinase-like	93	FSCACGAITTTK	2	51	2	7%

					LVDDHSVLEDEGK	2	80		
	PRid000003765	Artch_CL1553Contig1		92	YACACGAITTTK	2	49	2	7%
					IVDDHSVLEDEGK	2	80		
	PRid000071067	HelAn_TC39787	FBP aldolase	85	ALQNTCLK	2	34	3	7%
					ASANSLAQLGK	2	82		
					SAAYYQQGAR	2	37		
579	PRid000001782	Artch_CL430Contig1	Cysteine synthase	352	TPMVYLNDIAK **Deamidated (NQ)**	2	63	9	30%
					IGNSMIADAEER **Deamidated (NQ)**	2	87		
					IGNSMIADAEER	2	32		
					LIAVVFPSFGER	2	52		
					YLSTILFQSIR	2	59		
					VDIFVAGIGTGGTISGVGR	2	108		
					VHYETTGPEIWEDTK x 2	2	64		
					SILVEPTSGNTGIGLAFIAASK	2	105		
					AEEIVNSTPHAYMLQQFDNPANPK	3	49		
	PRid000019397	LacSat_TC16280		311	TPMVYLNDIAK	2	63	4	20%
					AFGADLVLTDSSK x 2	2	98		
					VDIFVAGIGTGGTISGVGR	2	108		
					SILVEPTSGNTGIGLAFIAASK	2	105		
591	PRid000000556	Artch_CL2057Contig1	Quinone oxidoreductase	266	SLGADEVLDYK	2	73	8	41%
					IEAASINPIDYK	2	85		
					VVSTLGGAGGGLAEYTVAK	2	103		
					LMQAVWYTSYGGGAAGLK	2	77		
					FPFIPVGDVAGEVVEVGPGVK	3	63		
					KFPFIPVGDVAGEVVEVGPGVK	3	49		
					VIDITPSGGTFWHYAVNTITFSK	3	31		
					ESSTVSRPPEVSAADGASLVVAGCTALHALTTSCGLK	4	27		
622	n.i.	n.i.	n.i.	n.i.	n.i.		n.i.	n.i.	n.i.
639	PRid000022848	LacSat_TC19731	ADH (glutathione-dependent formaldehyde dehydrogenase)	62	VQILFTALCHTDAYTWSGK	3	62	2	11%
					GWGTSVIVGVAASGQEISTRPFQLVTGR	4	27		
659	PRid000051801	LacSer_TC2861	FBP aldolase	93	LASIGLENTEANR	2	68	2	10%
					YAAISQDNGLVPIVEPEILLDGEHGIDR **Deamidated (NQ)**	3	61		

	PRid000075333	HelAn_TC44053		84	LASIGLENTEANR	2	68	2	11%
					TLLVTPPGLGNYISGAILFEETLYQSTVDGK	3	50		
690	PRid000002071	Artch_CL1487Contig1	Ferredoxin-NADP reductase	125	DPNATVIMLATGTGIAPFR	2	84	3	23%
					DPNATVIMLATGTGIAPFR **Oxidation (M)**	2	47		
					GVCSNFLCDLKPGSEVQITGPVGK	3	63		
	PRid000021515	LacSat_TC18398		121	**EGQSIGVIPDGIDPK**	2	59	3	11%
					DPNATVIMLATGTGIAPFR	2	84		
					DPNATVIMLATGTGIAPFR **Oxidation (M)**	2	47		
751	PRid000002024	Artch_CL1318Contig1	Xyloglucan endotransglucosylase	143	TGQPYSVQTNVYAHGK x 2	2	56	2	12%
					AIQLILDQNSGCGFASK x 2	2	122		
753	n.i.	n.i.	n.i.	n.i.	n.i.		n.i.	n.i.	n.i.
813	PRid000001382	Artch_CL5528Contig1	Voltage-dependent anion channel	112	TIFSFVVPDQR	2	75	2	9%
					LCTTITIDEPAPGLK	2	74		
839	n.i.	n.i.	n.i.	n.i.	n.i.		n.i.	n.i.	n.i.
840	PRid000005276	Artch_CL1021Contig1	Carbonic anhydrase	96	APFDPVER	2	38	5	24%
					NVANMVPPYNQTK	2	41		
					VCPSVVLDFQPGEAFVVR	2	87		
					VLAEHGSTSVDDQCVQCEK	3	46		
					GLMSFPDEGPHTTDFIEDWVK	3	28		
848	PRid000001996	Artch_CL1212Contig1	Acidic endochitinase	74	VFLSLGGQNGR	2	74	1	3%
886	PRid000000494	Artch_CL1827Contig1	cytosolic triose phosphate	537	FFVGGNWK	2	38	10	48%
			isomerase		VAYALSQGLK	2	62		
					IIYGGSVSGSNCK	2	97		
					VIACVGETLEQR	2	93		
					EAGTTMEVVAAQTK x 2	2	90		
					ALLNETNEFVGDK	2	72		
					EAGTTMEVVAAQTK **Oxidation (M)**	2	77		
					VASPAQAQEVHAGLR x 2	2	64		
					WFQENISADVAATTR x 2	2	116		
					ISSWDNVVLAYEPVWAIGTGK x 2	2	91		
942	n.i.	n.i.	n.i.	n.i.	n.i.		n.i.	n.i.	n.i.
956	n.i.	n.i.	n.i.	n.i.	n.i.		n.i.	n.i.	n.i.

982	n.i.	n.i.	n.i.	n.i.	n.i.		n.i.	n.i.	n.i.
985	n.i.	n.i.	n.i.	n.i.	n.i.		n.i.	n.i.	n.i.
996	PRid000001185	Artch_CL4694Contig1	Photosystem I	114	TRYPVVVR	2	43	3	26%
					GVGSVVTVDQDPK	2	86		
					VNYANVSTNNYALDEIEEVA	2	58		
1212	n.i.	n.i.	n.i.	n.i.	n.i.		n.i.	n.i.	n.i.
1219	PRid000081646	HelAn_TC50366	Oxygen evolving complex 33 kDa	164	VPFLFTIK	2	34	6	28%
			photosystem II protein		GGSTGYDNAVALPAGGR	2	84		
					DGIDYAAVTVQLPGGER	2	87		
					ELVATGKPESFGGNFLVPSYR	3	27		
					GTGTANQCPTIEGGVNGFAVKPGK	3	39		
					GGSTGYDNAVALPAGGRGDEEELLK	3	61		
	PRid000004906	Artch_CL6319Contig1		138	VPFLFTIK	2	34	6	42%
					GGSTGYDNAVALPAGGR	2	84		
					GTGTANQCPTIEGGVDGFAVK	3	66		
					QLVASGKPESFGGEFLVPSYR	3	32		
					GGSTGYDNAVALPAGGRGDEEELLK	3	61		
					ITLSVTSSKPDTGEVIGVFESIQPSDTDLGAK	3	32		

Legend:

in BOLD RED are evidenced differential peptides among orthologs

n.i. stands for not identified spots